Transportation Geotechnics 22 (2020) 100299

Contents lists available at ScienceDirect

Transportation Geotechnics

journal homepage: www.elsevier.com/locate/trgeo

Geocellular railway drainage systems: Physical and numerical modelling

Ali Tasalloti[a], Alec M. Marshall[b,*], Charles M. Heron[b], Mir Amid Hashemi[b]

[a] Department of Civil and Natural Resources Engineering, University of Canterbury, Christchurch, New Zealand
[b] Nottingham Centre for Geomechanics, Faculty of Engineering, University of Nottingham, University Park, NG7 2RD, United Kingdom

ARTICLE INFO

Keywords:
Railway drainage
Physical model
Numerical model
Rainfall simulation

ABSTRACT

The importance of resilient railway infrastructure is paramount when considering the increased likelihood of extreme weather and flash flood events in coming years. One of the main causes of instability of railway tracks is excess water in the trackbed, particularly when it is at or above the interface of the ballast and subgrade. Conventional drainage systems are susceptible to clogging and deterioration. Resilient track drainage systems should therefore have sufficient capacity to allow water to dissipate quickly, but they should also be designed to ensure long-term operation with minimal or easily performed maintenance. This paper presents results from an investigation of a potential new railway drainage system using geocellular components. In the paper, the development of a large scale physical model is described which represents a full scale unit cell of a sleeper-to-sleeper track substructure. The physical model includes ballast and subgrade layers, under-track and lateral drainage systems, rainfall simulation, and instrumentation. Results demonstrate the relative hydraulic response of the drainage system with and without the geocellular components. The paper also describes the development of a numerical model of the track subgrade and drainage system, which was first calibrated and verified using experimental data from the physical model, then extended to study the effect of certain parameters on the hydraulic response of the railway track. Results indicate that the under-track geocellular drainage system offers potential benefits in terms of maintaining a lower water table level within the subgrade as well as in aiding the migration of fines out of the ballast.

Introduction

The long-term performance and overall safety of railway infrastructure are critically dependent on the drainage capacity of the track system. Railway drainage system modernization is considered a key factor for improving railway network safety and capacity and enhancing the resilience of railway infrastructure. Accumulation of water within the track substructure reduces the shear strength and stiffness of the subgrade layer and may cause excessive trackbed settlement under train loading which ultimately results in speed limitations for trains and/or discomfort for passengers [4,13,21,23]. Water is accumulated in the track system through rainfall and run off events as well as groundwater seepage. Water accumulation causes accelerated deterioration of trackbeds and leads to more frequent maintenance requirements, including ballast cleaning and undercutting operations. This inevitably results in significant costs to the end-user of the railway. Considering the anticipated adverse effects of climate change in coming years (e.g. more extreme weather and flash flood events), the need for resilient railway infrastructure is paramount.

Although the significance of an adequate ballast drainage system is widely recognized [1,6,18,22,27], the role of subgrade characteristics in the drainage performance of the railway infrastructure is often neglected in design and practical applications. Previous research studies have shown that the permeability and mechanical behaviour of ballast decreases considerably once it is contaminated with “fines” (i.e. particles smaller than ~0.06 mm) [12,14,15,18,19,24]. For example, in a series of tests with different degrees of fouled ballast, it was shown that permeability dropped from 0.3 m/s for clean ballast to 5×10^{-5} m/s for a fouled ballast with a fouling index of 40% [18]. Studies have also shown that the subgrade plays an important role in enabling drainage of water from the track system [7,8,11,20,28].

There are various mechanisms of failure associated with the track drainage system, such as internal failure (i.e. ballast fouling), external failure (i.e. clogging of drainage pipes), as well as mechanisms associated with the subgrade [11]. An illustration of the track and drainage system and the factors associated with railway track failures is provided in Fig. 1. In practice, the failure of drainage systems has mainly been observed in areas where the subgrade layer has a relatively low

* Corresponding author.
E-mail addresses: ali.tasalloti@canterbury.ac.nz (A. Tasalloti), alec.marshall@nottingham.ac.uk (A.M. Marshall), charles.heron@nottingham.ac.uk (C.M. Heron), amid.hashemi@nottingham.ac.uk (M.A. Hashemi).

https://doi.org/10.1016/j.trgeo.2019.100299
Received 27 August 2019; Received in revised form 6 November 2019; Accepted 7 November 2019
Available online 13 November 2019

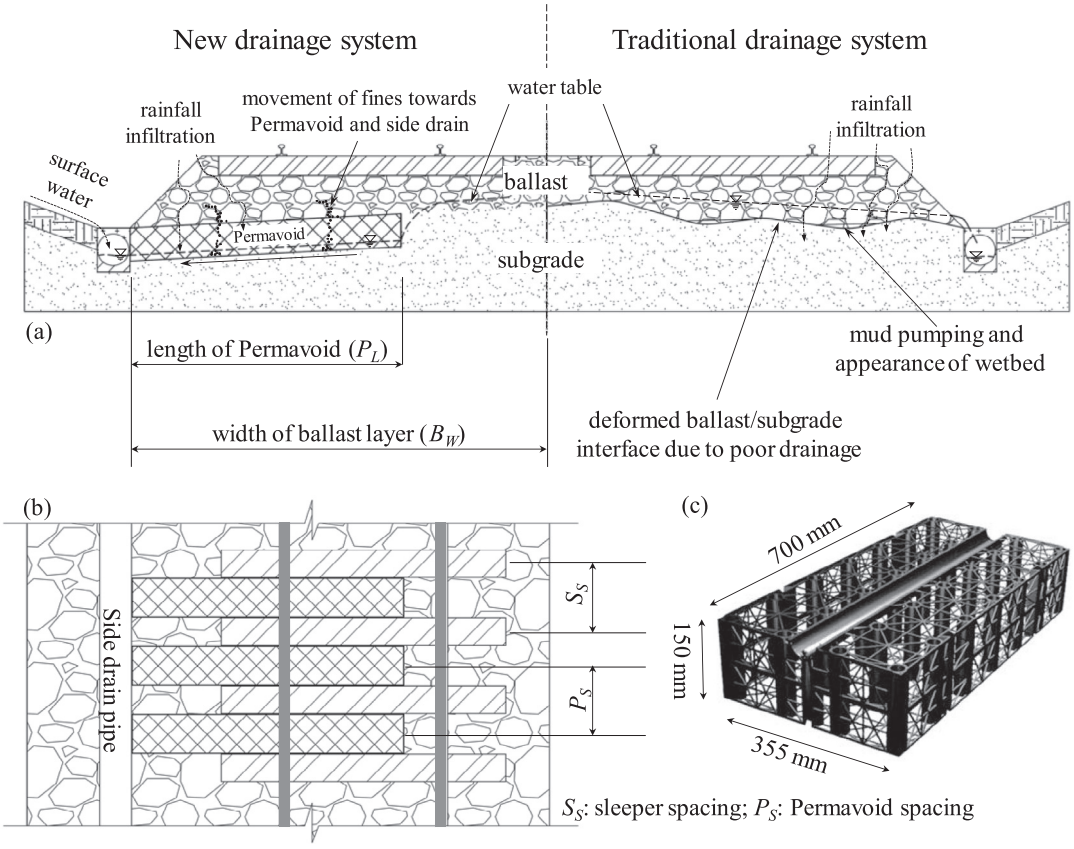

Fig. 1. An overview of railway drainage system investigated in this paper: (a) cross-section view of railway track and comparison between new and traditional drainage systems, (b) plan view showing spacing between sleepers and Permavoid, and (c) 'Permavoid' geocellular system component (image courtesy of Wrekin Products).

permeability [15,18]. In this condition, longer times are required for water to reach the side drainage pipes. Providing effective under-track drainage paths can address this issue and ensure that the water table remains within the subgrade formation. Maintaining water levels within the subgrade also reduces the possibility of mud pumping, which can occur when the water table is close to the ballast-subgrade interface [3,7,8,25]. When the water table is below the subgrade-ballast interface, the subgrade may be in an unsaturated state, which will affect the hydraulic and mechanical response of the layer [2,5]. The effect of an unsaturated subgrade on the hydraulic and mechanical response of a railtrack has not been studied in detail.

Currently, there are a limited number of practical solutions adopted to improve railway track drainage, such as sand blankets or a geocomposite layer between the subgrade and ballast [21,9]. However, these solutions all suffer, to varying degrees, from long-term performance issues, such as susceptibility to clogging and maintenance difficulties.

This paper presents results obtained from a research project investigating new approaches to drainage within the railway system. The paper focuses on results related to a geocellular drainage system known as 'Permavoid' (Fig. 1c). Fig. 1 shows the main aspects of the study, including parameters related to the location and length of the Permavoid units within the track structure (Fig. 1a), and their spacing in the longitudinal direction (Fig. 1b). The relative performance of the drainage system was evaluated using a combination of physical and numerical modelling approaches, with the obtained experimental data used to verify the outcomes of the numerical model. A physical model was developed to represent a full scale unit cell of a sleeper-to-sleeper track substructure. The model is capable of accommodating subgrade and ballast layers, under-track and trackside drainage components, and rainfall simulation using a set of spray nozzles. Changes in water table level and the migration of fine particles are captured visually through transparent acrylic windows along one side of the model container, whilst water pressures within the subgrade are measured using pore pressure transducers (PPTs) and standpipes (SPs). The physical model was used to study the hydraulic response of the track system only; mechanical loading was not included. Whilst the physical model may not fully represent all aspects of problematic railway drainage scenarios, the model is able to provide a quantitative evaluation of the relative response of different drainage scenarios. As a means of verification, the numerical model was first used to replicate the physical model, including consideration of unsaturated flow, and then extended to evaluate the effect of a wider range of model parameters (e.g. drainage length across and spacing along the track).

Physical model

The physical model, illustrated in Fig. 2, was constructed using marine plywood coated with layers of liquid latex and supported within a steel frame. The model measures 4880 mm in length (representing half of a double-track railway), 620 mm in width (representing a sleeper-to-sleeper centre spacing), and 1220 mm in height (accommodating ballast and subgrade layers). Longitudinal drainage along the railway track was also included in the box, with an outlet at one of the long sides. Five acrylic windows were installed on the front side of the box to visually monitor the water table variation during rainfall, as shown in Fig. 2. These windows cover the ballast and subgrade layers and also the location around the drainage pipe along the railway track. The windows provided valuable visual information on the movement of fines within the ballast and Permavoid units during simulated rainfall.

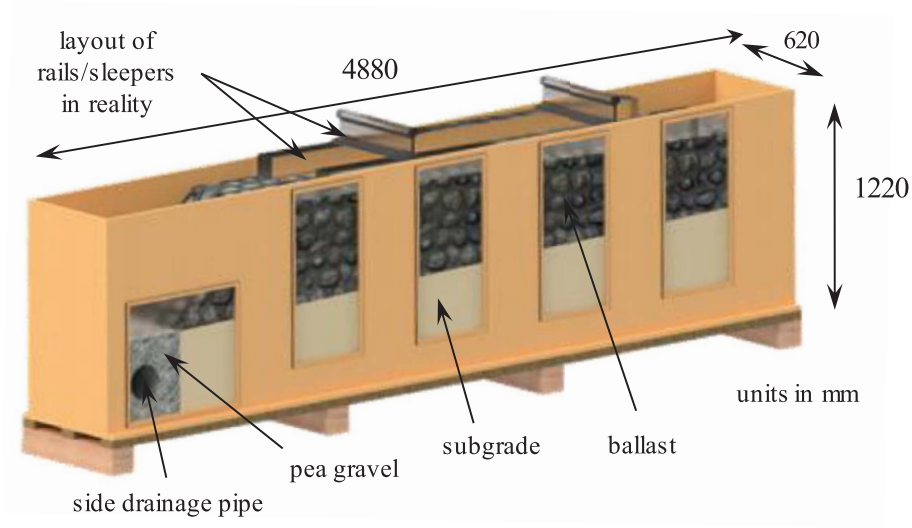

Fig. 2. Graphical view of physical model: front view showing acrylic windows and various layers.

Rainfall intensity

The hydraulic response of a railway system is influenced by the rainfall duration and its intensity, or more specifically the ratio of rainfall intensity to the permeability of the system. In order to simulate realistic rainfall events in this study, intensity-duration–frequency (IDF) curves for the UK were established using hourly rainfall data from 26 gauges across the UK (data provided by the Centre for Environmental Data Analysis), as illustrated in Fig. 3. The gauges were selected based on their proximity to a main railway network within the UK (eliminating extreme rainfall events in mountainous areas). A statistical analysis following Gumbel theory [10] was performed to establish the IDF curves for return periods of 2, 5, 10, 25, 50, and 100 years. The minimum and maximum IDF curves for different rainfall durations were then established, as shown in Fig. 4. Depending on the return period and duration, rainfall intensities are in the range of 5–260 mm/h. Network Rail standard NR/L3/CIV/005/2A [17] recommends that the track drainage system should be designed for rainfall events for a return

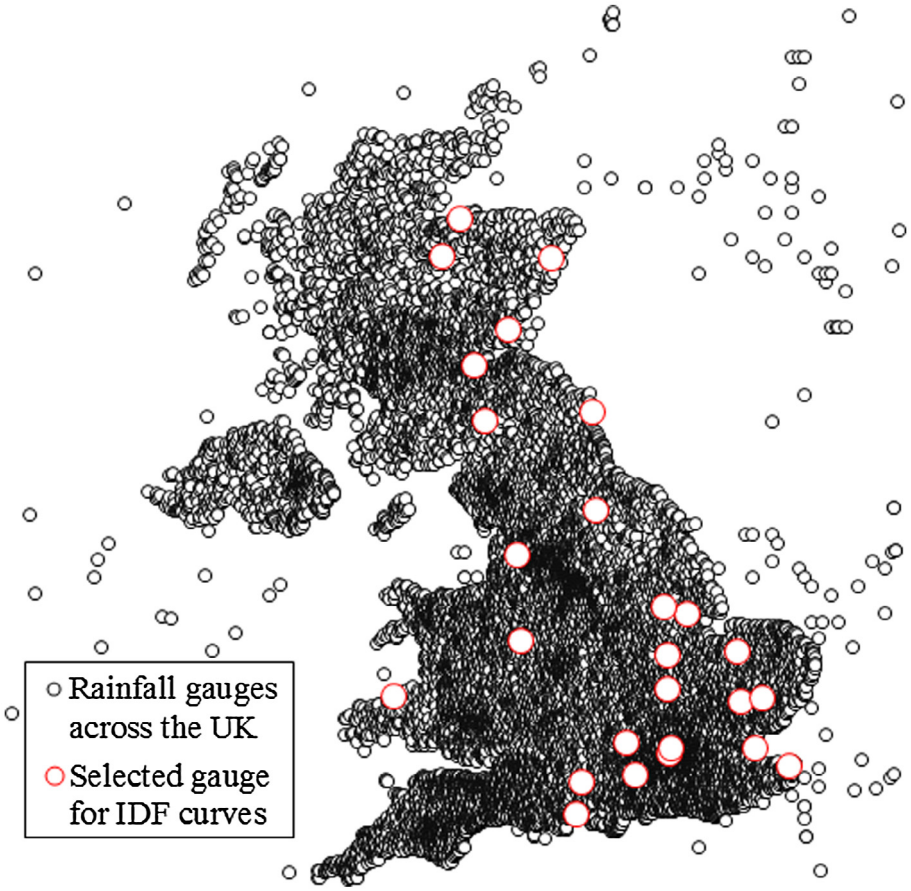

Fig. 3. Location of the 26 rainfall gauges for the establishment of IDF curves.

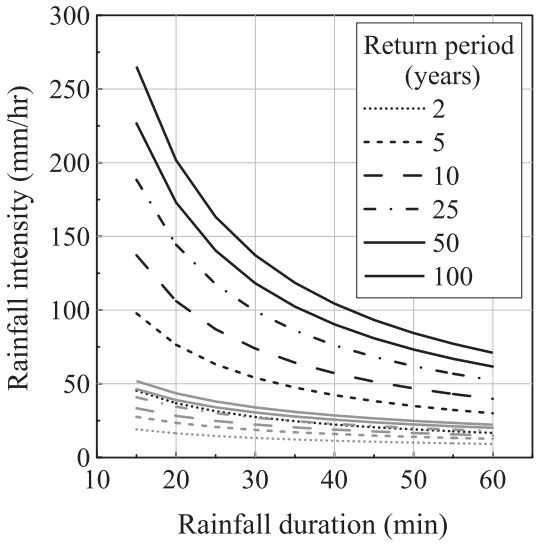

Fig. 4. IDF curves (minimum in grey and maximum in black) for rainfall events from selected gauges for different return periods.

period of 50 years, hence, by assuming a rainfall duration of 30 min, an intensity of 135 mm/h was chosen for the physical model. It should be noted, however, that during experiments, rainfall durations of greater than 30 min were used in order to reach a steady state condition.

The physical model used eight 1.2 mm aperture, 90° spray nozzles to simulate rainfall, as shown in Fig. 5. The pattern for the nozzles was designed to achieve a uniform intensity over the area of the box without excessive overlap of coverage area. The nozzles were placed 310 mm above the ballast, except near the sloped ballast adjacent to the side drain, where this distance varied somewhat, resulting in some variation to the rainfall coverage in this area. A branched pattern of pipes was used for the water supply to ensure uniform pressure/flow at each nozzle. The system is capable of providing rainfall intensities in the range of 70–152 mm/h, enabling low and high rainfall intensity simulation with one set of nozzles. Fig. 5 also shows the location of the pore pressure transducers (PPTs) and standpipes (SPs) used in the physical model.

Materials and instrumentation

The hydraulic properties of the ballast and subgrade layers are important considerations. Clean ballast generally has a permeability that is orders of magnitude greater than the subgrade (at least in areas where drainage is a problem), however ballast contamination can significantly reduce its permeability. A wide range of soil types can be encountered in the subgrade. Previous studies [15,18] indicated that, in areas where railway tracks are constructed on relatively low permeability subgrade, the chance of track closure due to drainage failure is relatively high (i.e. “problem areas”). This is mainly due to the significant influence of moisture content on the resilient modulus of the subgrade soil. The selection of the subgrade soil for the physical model was therefore challenging. On one hand, the material should be relatively easy to compact since a large amount of material was required for the model (nearly 2500 kg); clay content should therefore be limited (< 10%). On the other hand, the permeability of the subgrade layer should be low enough to be representative of “problem areas”. Considering these constraints, a fine sand (50%) with silt (45%) and some fraction of clay sizes (< 5%) was chosen for the subgrade. The material was obtained from Rotherham Sand & Gravel (RSG) in Sheffield, UK,

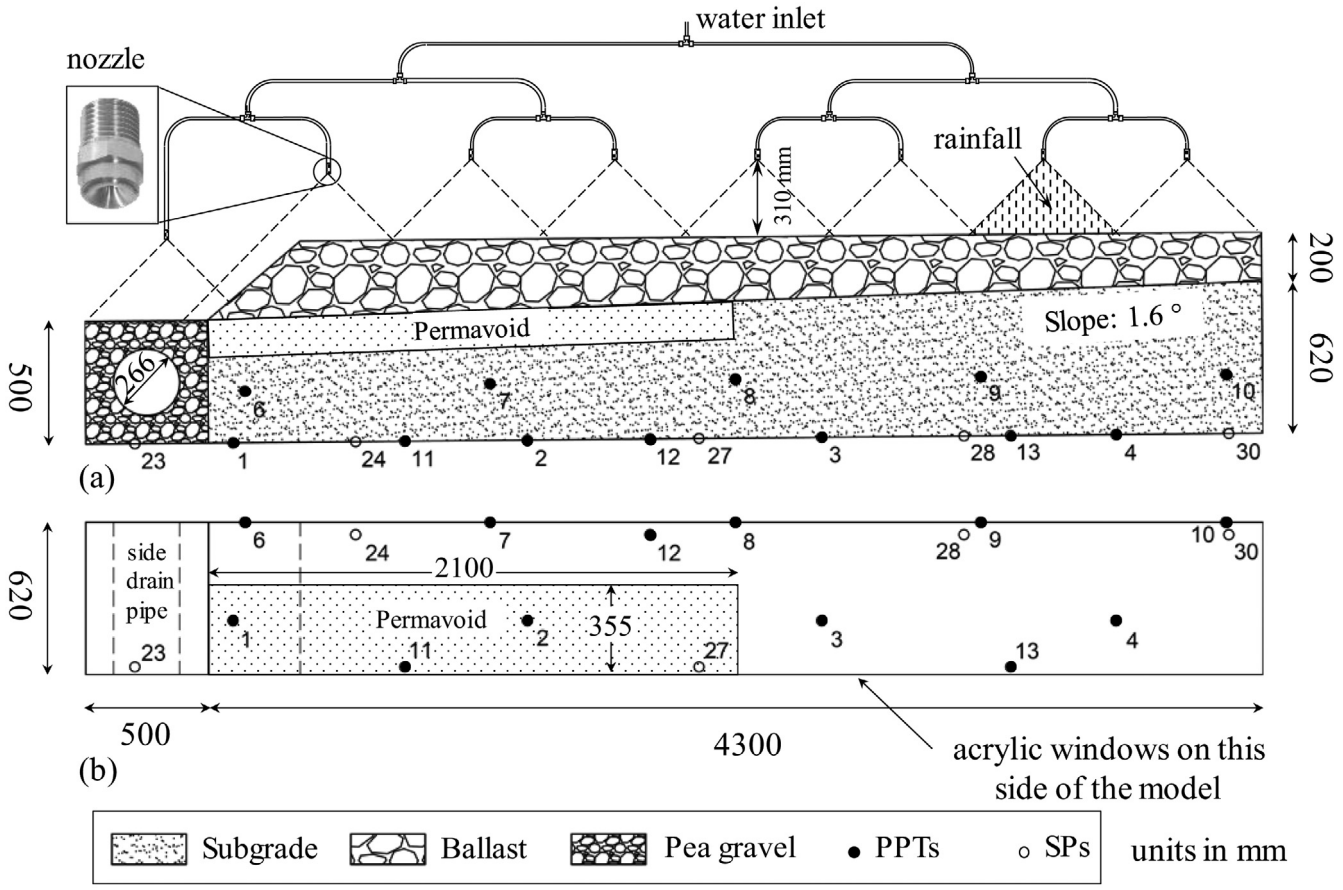

Fig. 5. Physical model illustrating rainfall simulation system and location of PPTs and SPs: (a) cross section and (b) plan view.

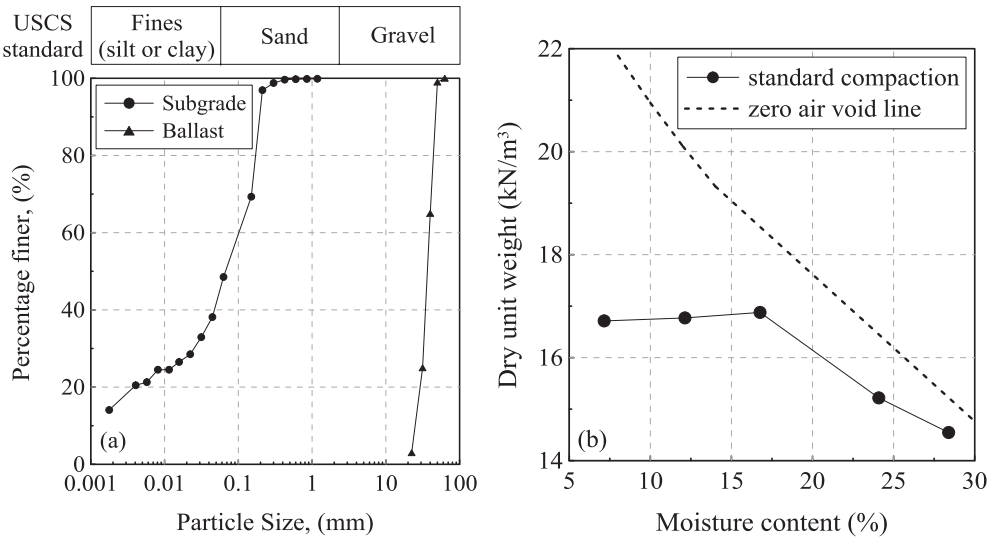

Fig. 6. (a) Particle size distribution of ballast and subgrade layers, and (b) compaction curve of subgrade material.

and is a by-product of the washing process of quarry aggregate. Fig. 6(a) illustrates the particle size distribution (PSD) of the selected subgrade material and the ballast. The results of standard compaction tests on the subgrade material are presented in Fig. 6(b). The index properties of the subgrade are: specific gravity $G_s = 2.65$, optimum moisture content $w_{opt} = 17\%$, dry unit weight $\gamma_{dry} = 16.8\,\text{kN/m}^3$ (compacted at w_{opt} with standard proctor energy), and saturated permeability $k_{sat} = 2 \times 10^{-7}$ m/s (the effect of a lower subgrade permeability is considered in Section 'Permeability of subgrade').

The 'Permavoid' geocellular system tested within the physical model had individual component dimensions of 700 × 355 × 150 mm, as shown in Fig. 1. These units are widely used for residential applications such as parking areas, houses, and golf courses. The mechanical performance of these drainage components under railway track loading, and in particular cyclic loading, is also an important consideration, however it is outside the scope of this paper. The effect of Permavoid on the stiffness of ballast under cyclic loading is reported in [26].

In order to capture the variation of water table over time within the physical model, a total of 17 pore pressure transducers (PPTs) and standpipes (SPs) were installed on the bottom and back side of the box, as shown in Fig. 5. PPTs were installed at location numbers 1–13 and SPs were located at the rest of the points.

Model preparation and testing procedure

The subgrade material was first air-dried from its natural state to reach 15–17% moisture content (to allow easier compaction) and then compacted inside the box in 50 mm layers using an electro compactor plate to reach a dry density of approximately 15 kN/m^3. The ballast was then placed on top of the subgrade layer. Note that the subgrade material layer was only prepared once; it was not re-prepared for each test. For the fouled ballast tests, a fouling index (FI) of 40, representing fouled to heavily fouled ballast [23], was achieved by manually mixing the subgrade material with ballast at a dry weight ratio of 40:60 (subgrade:ballast). For models that included the Permavoid components, the ballast layer was removed and half the length of the subgrade layer (~2.1 m) was excavated such that three Permavoid units could be placed at the ballast-subgrade interface. Before commencing rainfall simulation, all PPTs, SPs, pipes and connections were saturated with deaired water to ensure accurate and immediate response of the instruments.

Prior to the first test, the simulated rainfall was initiated and left to run until the response of the PPTs and SPs, and also the flow from the side drain pipe, indicated a steady state condition had been reached. The rainfall was then stopped and the model was allowed to drain. Between all tests (i.e. after rainfall and draining), the water table stabilized at a level between the bottom of the box and the base of the side drain pipe, with pore suctions keeping some amount of water within the subgrade layer above the water table (i.e. in an unsaturated condition). The model was left in this condition between each successive test. There was some variability of the level of the initial water table at the start of the tests, which impacted on the initial increase ("lift-off") of pressures, as seen in Fig. 7. This did not have a significant impact on data interpretation, as the focus was mainly on the steady state levels and water pressure response after rainfall (these were the key elements used in the calibration of the numerical model).

Four physical model experiments were conducted to evaluate the effect of the Permavoid drainage units on the hydraulic behaviour of the railway track system, as summarised in Table 1. Clean and fouled ballast conditions were tested, both with and without the Permavoid drainage units. The subgrade layer was in an unsaturated condition before commencement of the simulated rainfall, giving the subgrade a very low permeability. Therefore, to reach the steady state condition, a

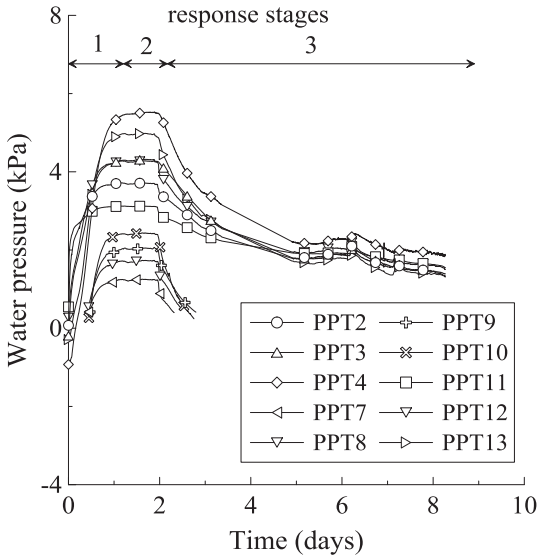

Fig. 7. Results of physical model for the condition of clean ballast with Permavoid.

Table 1
Summary of physical model tests.

Test label	Drainage detail	Ballast condition	q (mm/hr)	Rainfall duration (days)	q/k_{sat}
ND-Clean	Subgrade only	Clean	135	1	187.5
ND-Fouled	Subgrade only	Fouled (FI = 40)	135	1.5	187.5
PV-Clean	Subgrade and Permavoid	Clean	135	2	187.5
PV-Fouled	Subgrade and Permavoid	Fouled (FI = 40)	135	3	187.5

ND = No Drainage unit; PV = Permavoid drainage unit included; FI = Fouling Index according to [23], q = Rainfall intensity; k_{sat} = saturated permeability of subgrade.

high rainfall duration was required.

Results and discussion

Physical model

An example of the PPT response over time is shown in Fig. 7 for test PV-Clean (clean ballast with Permavoid). It should be noted that the PPTs were only able to measure positive pore water pressures, hence PPTs on the side of the container (PPT 7, 8, 9, and 10) only recorded data once the water table was higher than their elevation. Since the rainfall intensity is much greater than the infiltration capacity of the subgrade (as presented in Table 1), the excess water was shed off the ballast-subgrade interface towards the side drainage (i.e. pea gravel). Due to the relatively high permeability of the pea gravel compared to the subgrade, water initially infiltrated into the pea gravel and accumulated under the side drainage pipe and then infiltrated horizontally towards the subgrade layer from left to right. Thus, PPTs located closer to the pea gravel (i.e. PPTs 2 and 3; refer to Fig. 5 for PPT locations) initially responded to the rainfall infiltration, followed later by PPTs further from the side drain (i.e. PPT 4), as shown in Fig. 7. Concurrent to the horizontal infiltration of water from the pea gravel into the subgrade, water at the ballast-subgrade interface percolated downwards to the subgrade layer. These two mechanisms (i.e. horizontal and vertical infiltration) resulted in the accumulation of water from the base of the box until the subgrade layer became (nearly) saturated and a steady state was reached.

In Fig. 7, three stages of water pressure response are observed. Since the subgrade was initially in an unsaturated condition (i.e. the water table was located either at the invert of the lateral drainage pipe or near to the bottom of the box), there is a transient flow condition during which time the saturation level of the subgrade increases, finally reaching a steady state at the end of stage 1. During the steady state condition in stage 2, the inflow rate (i.e. rainfall intensity) is equal to the outflow, hence there is no change in water pressures. Upon stopping the rainfall (start of stage 3), the water pressure dissipates and water drains from the box through the outlet pipe, with degree of saturation in the subgrade layer decreasing over time.

Fig. 8 compares the water table levels at steady state from the four physical model experiments and demonstrates the influence of the Permavoid drainage units. For the tests without Permavoid with clean ballast (ND-clean), in most areas the water table was very close but slightly below the ballast-subgrade interface, whereas for the fouled ballast tests (ND-Fouled), the water table was slightly above the ballast-subgrade interface (i.e. within the fouled ballast layer). In a real train loading scenario, this would result in the possibility for mud pumping to occur [3,7,8,25]. On the other hand, for tests with Permavoid (PV), the water table was maintained well below the ballast-subgrade interface, even for the fouled ballast test (PV-Fouled). Although the Permavoid units were only placed along half of the subgrade length, their influence on the water table was significant up to the right side boundary of the physical model, which represents the plane of symmetry of a double-track system. These results indicate that the Permavoid drainage units maintain an unsaturated condition of the subgrade at the ballast-subgrade interface, with beneficial effects related to the occurrence of mud pumping and overall strength/stiffness of the track system.

An important drainage performance parameter is the time it takes to reach steady state (t_{ss}); a greater time to reach steady state condition indicates a longer rainfall duration required before track flooding issues arise. Based on the recorded data, t_{ss} for clean ballast without Permavoid (ND-Clean) was 1.7 h, whereas it was 28.9 h for clean ballast with Permavoid (PV-Clean). This significant increase in t_{ss} demonstrates the beneficial influence of Permavoid on the hydraulic response of the railway track. For the fouled ballast situation, t_{ss} was 36 and 18.9 h for with Permavoid (PV-Fouled) and without Permavoid (ND-Fouled) tests, respectively.

Visual observations through the acrylic windows of the physical model indicated that the Permavoid units retained fines washed out of the fouled ballast layer and directed a portion of these fines towards the side drainage. Fig. 9(a) (i.e. without Permavoid) shows that the fines moved from the fouled ballast layer towards the ballast-subgrade interface, effectively moving the interface upwards into the original ballast layer. As a result of the movement of the fines, the steady-state water table in test ND-Fouled was at a higher level compared to the clean ballast condition in test ND-Clean, as shown in Fig. 8. For tests

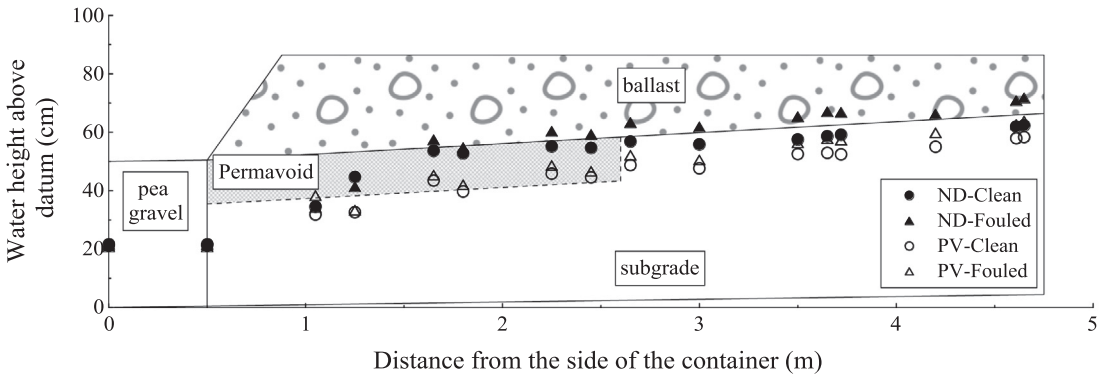

Fig. 8. Water table at steady state in four tests obtained in full scale physical model.

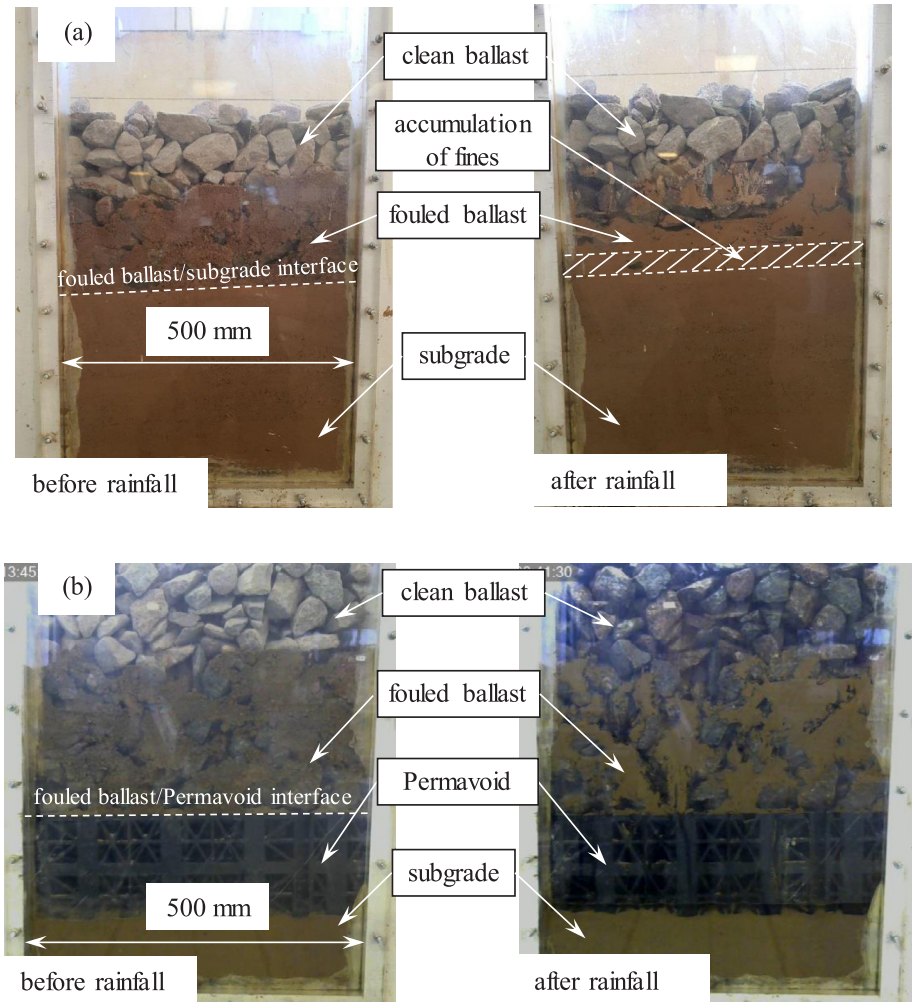

Fig. 9. The movement of fines under rainfall for fouled ballast conditions: (a) without Permavoid and (b) with Permavoid.

with Permavoid, Fig. 9(b) illustrates how the fines were able to move into the open structure of the Permavoid, with some of fines being washed towards the side drainage pipe. This is the reason why the steady-state water table results in Fig. 8 were similar for both the fouled and clean ballast tests with Permavoid.

Collectively, the physical model test outcomes suggest that, assuming a free-flowing side-drainage system exists, the use of an open-structure lateral drainage system (such as the Permavoid units) under the ballast will have significant beneficial influence on the hydraulic response of railway track, especially for a fouled ballast condition. It should be noted that the fouled ballast tests conducted here represent an extreme, instantaneous fouling of the ballast. In reality, if installed at the time of placement of clean ballast, the open-structure drainage units would also reduce the likelihood of the development of a fouled ballast layer, by assisting with the removal of fines moving downwards through the ballast, and by maintaining the water level below the ballast-subgrade interface, preventing mud-pumping (i.e. the upwards movement of fines). In addition, due to the versatile nature of these open-structure lateral drainage systems (e.g. Permavoid, which can be built according to specific design requirements, such as to fit between sleepers) it is feasible to install them in existing railway tracks, in particular during ballast cleaning and replacement. The open structure of the geocellular units should reduce the likelihood of clogging, however, if needed, the units could be maintained relatively effectively (e.g. jet washing through the ballast or via the side-drainage), contributing to the resilience of the trackbed drainage system.

Numerical model

A finite element method (FEM) numerical model was developed using the Abaqus software. The model was first calibrated and verified using experimental data, then used to evaluate the effect of parameter variations not considered in the physical model (e.g. length of Permavoid drainage units and spacing in the longitudinal direction along the railway track). The unsaturated soil hydraulic parameters (mainly for fouled ballast, pea gravel, and ballast) and the boundary conditions (both for rainfall infiltration and drainage elements) were the key factors considered during the calibration process. To reduce computational time, a 2D model was used for the cases where no Permavoid units were included (due to the symmetry of the model). For cases where the Permavoid was included, a 3D model was required, owing to the fact that the drainage units did not fully cover the width of the physical model (see Figs. 5 and 10).

The FEM simulations only considered hydraulic behaviour; the mechanical properties of all layers were ignored and all deformation were set to zero. The Van Genuchten [29] model was employed to capture the unsaturated soil hydraulic characteristics. The parameters of this model, described in Table 2, were used to establish the relationship between suction and degree of saturation, as illustrated in Fig. 11. The relationship between suction and degree of saturation (i.e. soil-water retention curve) shown in Fig. 11(a) was established by conducting a test on the subgrade material, compacted to the same density as in the physical model tests, using an unsaturated triaxial apparatus incorporating the axis translation technique [16]. In

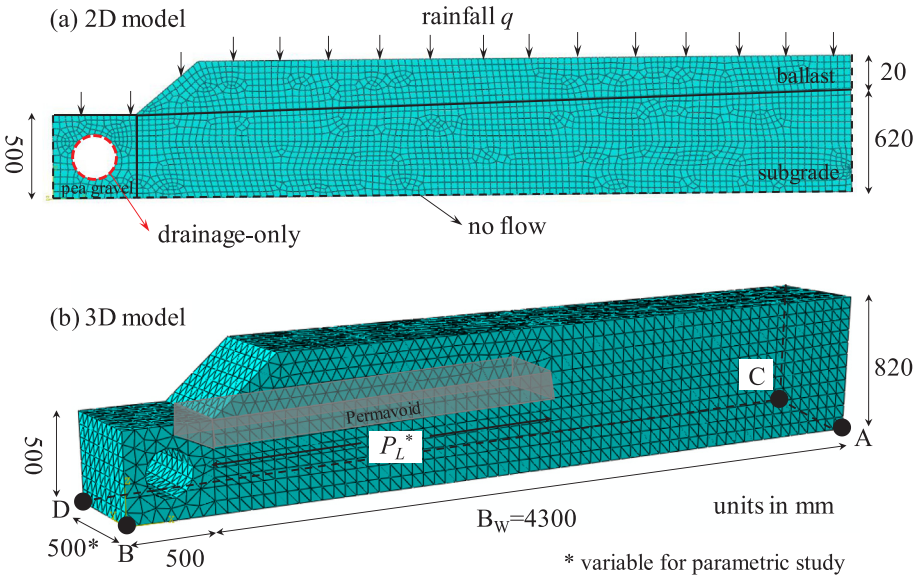

Fig. 10. FEM model discretization in (a) 2D and (b) 3D (including location of points A, B, C, and D).

Table 2
Calibrated FEM model hydraulic parameters derived from experimental results.

Layer	Saturated condition permeability	Unsaturated condition (Van Genuchten parameters)*			
	k_{sat} (m/s)	n	α (1/kPa)	θ_r	θ_s
Subgrade	2×10^{-7}	1.8	0.167	0.09	0.33
Ballast	0.3	2	14	0	0.4
Pea gravel	0.03	2	1.4	0	0.3
Fouled ballast	1×10^{-6}	2	0.17	0.09	0.33
Permavoid	3	–	–	–	–

* n and α are curve fitting parameters; θ_r is residual volumetric water content; θ_s is saturated volumetric water content.

addition, the ratio of unsaturated to saturated permeability (k_r) presented in Fig. 11, based on the Van Genuchten model, was adopted in the FEM analyses, with horizontal and vertical permeability assumed to be the same.

In the 2D model, a total of 2735 CPE8RP elements (8-node plane strain quadrilateral elements with pore pressure degree of freedom) were used. For the 3D model, a total of 32,267 element C3D4P (4-node linear tetrahedral elements with pore pressure degree of freedom elements) were used. The initial water table was set according to the values recorded by PPTs in the corresponding physical model test. Water flow was restricted at the left, bottom, and right boundaries, whereas a drainage-only boundary condition was prescribed around the side drainage pipe (i.e. water pressure not allowed to be greater than zero). Rainfall infiltration was simulated by surface inflow equivalent to the rainfall rate in the experiments. Due to the contrast in permeability at the ballast/subgrade interface, the mesh size and the numerical time increments were adjusted to ensure proper convergence of the model.

Figs. 12 and 13 show a comparison between the experimental pore water pressures and those from the FEM models at corresponding locations (illustrated in Fig. 5). The numerical model was able to capture the effect of unsaturated flow both during rainfall and once the rainfall was stopped. The main consideration relating to unsaturated flow is the dependency of subgrade permeability on degree of saturation, as shown in Fig. 11(b), which consequently influences the time-dependency of the pore water pressure response during and after rainfall. In the numerical models, the rate of increase in water pressure from start of rainfall and the rate of pressure dissipation (i.e. after rainfall) were similar to the recorded data; emphasis was placed on matching the numerical results to the post-rainfall experimental data, for reasons explained earlier relating to the variation of initial water table in the physical model tests.

Deviations between the numerical and physical model results may be attributed to several factors. One factor relates to the homogeneity of the soil within the physical model, especially the subgrade, which, due

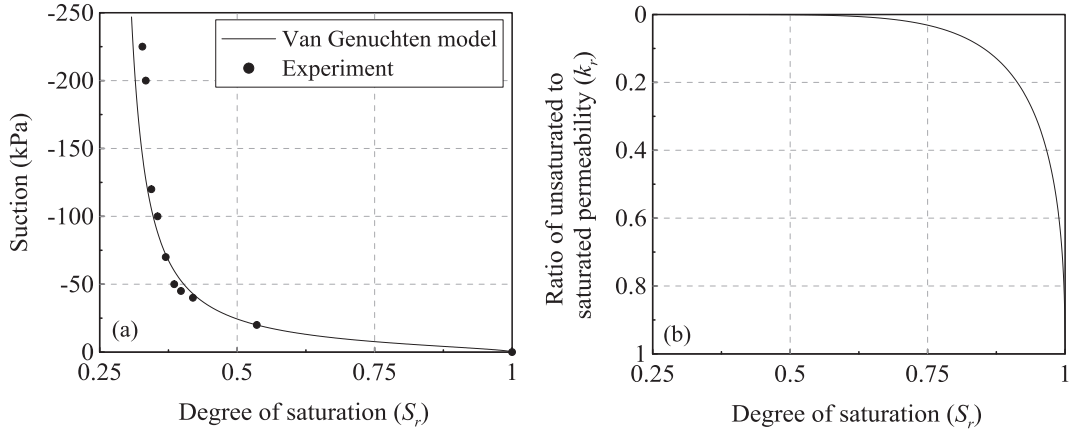

Fig. 11. (a) Soil water retention curve and (b) ratio of unsaturated to saturated permeability used in FEM analyses.

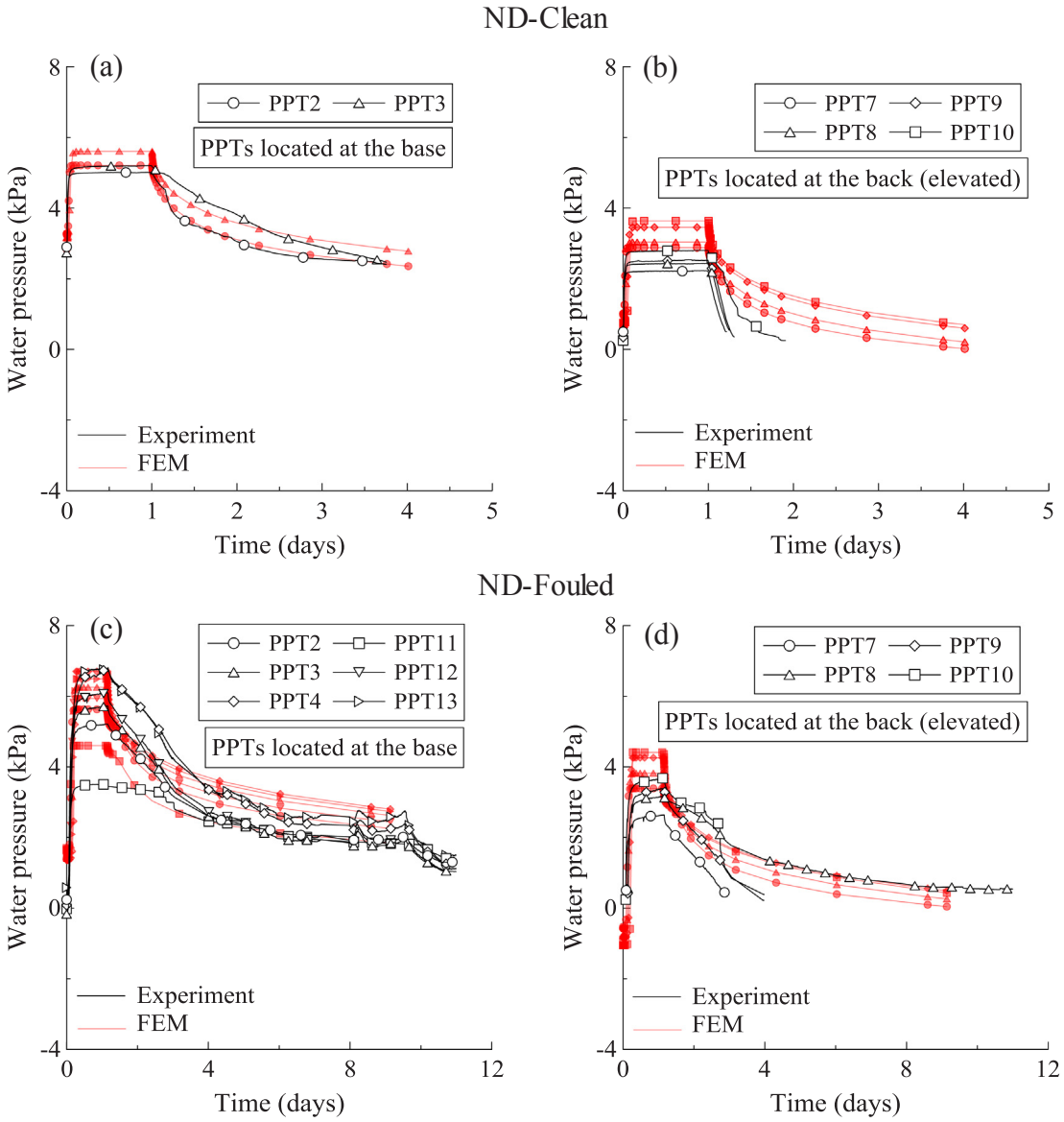

Fig. 12. Comparison between numerical model and experimental results for tests without Permavoid: (a and b) clean ballast (ND-Clean), and (c and d) fouled ballast (ND-Fouled).

to the preparation method, was not entirely homogeneous. Important parameters such as degree of saturation, saturated/unsaturated permeability, and void ratio were therefore not uniform within the physical model. This variation in parameters at a given time was not considered in the FEM models. Furthermore, even though all PPTs, SPs, and pipes were saturated with de-aired water prior to rainfall simulation, it is possible that air bubbles could have migrated into the pipes/instruments during tests, thereby affecting the measured responses (e.g. final value recorded by PPTs and rate of response to pressure changes).

A limitation of the numerical model relates to its ability to capture the effect of the movement of fine particles for tests with fouled ballast. In the physical model tests, once the rainfall was started, fine particles gradually moved towards the ballast-subgrade interface, and the thickness of this new layer increased until it reached a constant thickness. As this phenomenon could not be replicated in the FEM models, for simulation of these tests, based on visual inspections, the final thickness of the deposited fine particle layer that accumulated at the ballast-subgrade interface was considered as the initial condition in the FEM models. This limitation may also explain some of the deviation between experimental and numerical results observed in Figs. 12 and 13.

Overall, the agreement between the numerical model and experimental data was satisfactory; the FEM model was able to capture the unsaturated transition stage both during and after rainfall. In addition, including the Permavoid units was observed to decrease the maximum water pressures in both physical and numerical models, especially for fouled ballast tests (a reduction of 20% and 14% was observed in the physical and numerical models, respectively). The numerical outcomes again indicate the effectiveness of the Permavoid units in reducing water pressures in railway track (i.e. lowering the water table further below the ballast-subgrade interface). Comparison of numerical and physical model results gave sufficient confidence to carry out further parametric analyses with the numerical model (presented in the next section).

Parametric study

This section investigates, using the FEM models, several key factors affecting the hydraulic response of a railway track with lateral drainage (e.g. geocellular Permavoid units) that could not practically be studied

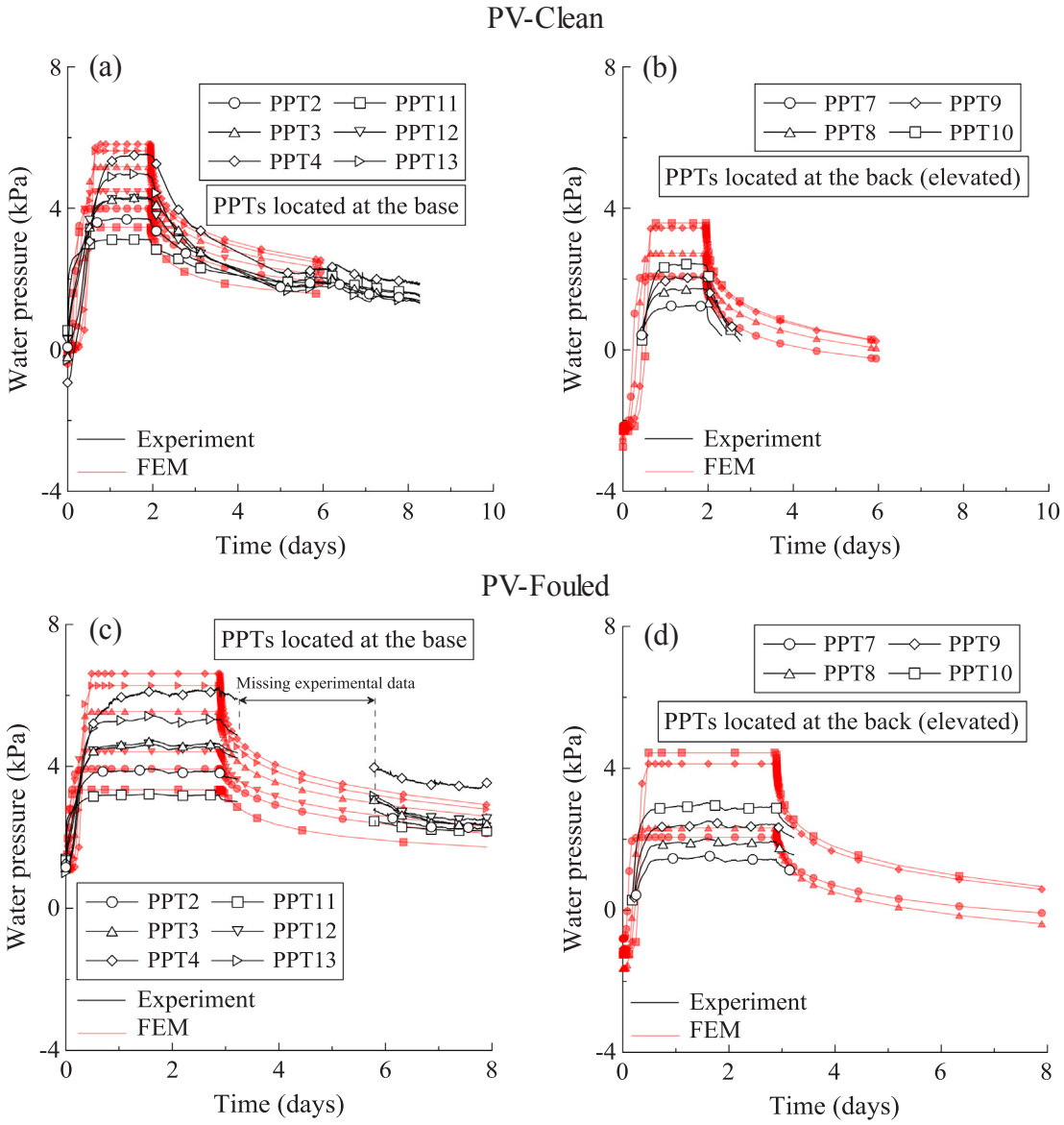

Fig. 13. Comparison between numerical model and experimental results for tests with Permavoid: (a and b) clean ballast (PV-Clean), and (c and d) fouled ballast (PV-Fouled).

with the physical model; relevant geometric parameters are illustrated in Fig. 1. In particular, the relative length of the drainage units compared to the width of the ballast (P_L/B_W), the spacing of the units relative to sleeper spacing (P_S/S_S), and the permeability of the subgrade are considered. The response of water pressures during and after simulated rainfall are compared at four locations within the model: points A, B, C, and D, as indicated in Fig. 10(b). The model parameters, element types, boundary conditions, and rainfall intensity were the same as the physical model tests, as detailed in Table 2.

Length of drainage units

In the FEM models investigating the relative length (P_L/B_W), the length P_L of the Permavoid drainage units was varied from 1.05 m to 4.3 m, resulting in P_L/B_W ranging from 0.25 to 1. In these analyses, it was assumed that the units were placed between sleepers (P_S/S_S = 1).

Fig. 14(a) illustrates the pore water pressure (PWP) at point A against time (i.e. at the plane of symmetry furthest from the lateral drainage, see Fig. 10). The results with no Permavoid are also plotted for comparison. The data illustrates that the maximum PWP at point A was nearly 5.7 kPa for all cases except P_L/B_W = 1.0, where it was 4.6 kPa (a reduction of 19%). The variation of P_L/B_W has a marginal influence on the maximum PWP, however it did have some influence on the rate of water pressure dissipation after rainfall. Fig. 14(b) shows that P_L/B_W has a significant effect on the elevation of the water table at steady state along the cross-section of the track (moving from B to A in Fig. 10). For a given distance to the side drainage, an increase in P_L/B_W results in a lower elevation of water table. Drainage unit lengths relating to P_L/B_W = 0.75 provide a considerable benefit to most of the area beneath the rails/sleepers, i.e. the areas most affected by train loading (from 1.5 to 4.0 m on the x-axis of Fig. 14(b)), where mud pumping is most likely to develop.

Spacing of drainage units

In the FEM models investigating spacing along the track, the spacing of the drainage units P_S in relation to sleeper spacing S_S was varied from 0.62 m (i.e. between every sleeper) to 2.48 m (between every 4th sleeper), with P_S/S_S ranging from 1 to 4. For these analyses, the relative length was kept constant at P_L/B_W = 0.50.

In Fig. 15, the elevation of the water table at steady-state along a line between points D and C is plotted. This line represents the mid-

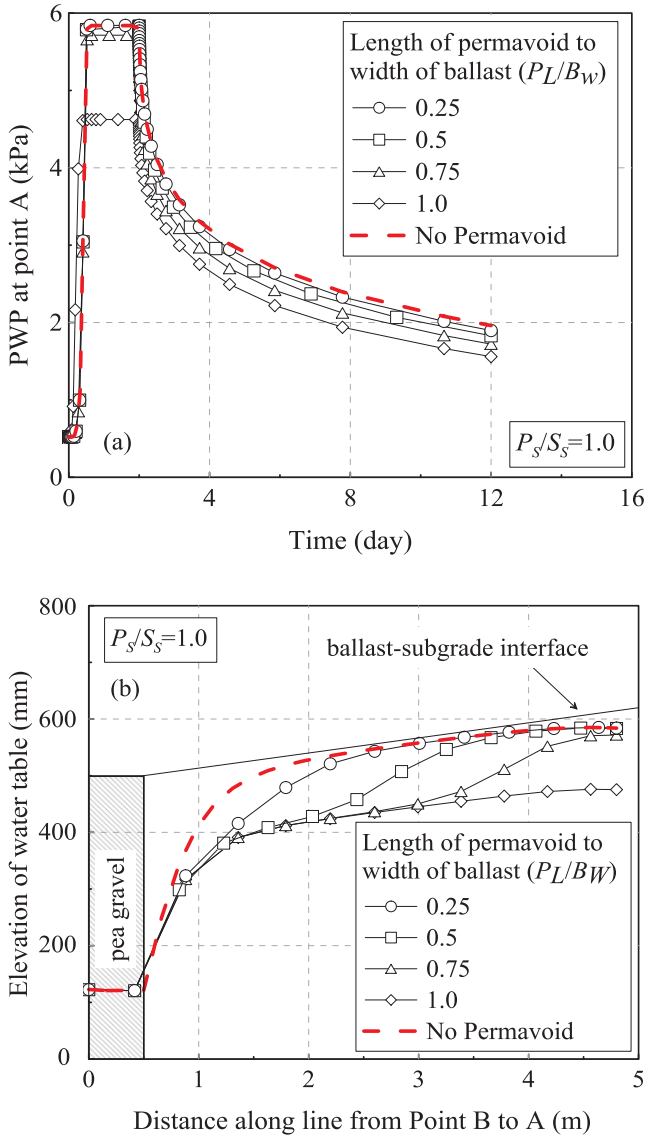

Fig. 14. Effect of P_L/B_W on (a) pore water pressure (PWP) at point A with time, and (b) steady-state water table level along line from point B to A.

point along the track between drainage units, hence it is the worst-case section in terms of water pressures. The data indicates that the drainage units have little effect at this location except for the case where they are placed between each sleeper (P_S/S_S = 1.0). This outcome suggests that, in order to achieve a significant benefit from the installation of lateral drainage units, they either need to be placed very close together (i.e. between every sleeper), or a continuous array of drainage units could be used along the track. As previously mentioned, the mechanical response of the drainage units and of a railway system incorporating such drainage systems still requires study.

Permeability of subgrade

In reality, subgrade permeability in problematic areas may be less than that simulated in the physical model (where saturated permeability $k_{sat} = 2 \times 10^{-7}$ m/s). To assess the effect of a lower subgrade permeability, Fig. 16 includes data of pore water pressure (PWP) at point A in FEM models having a saturated subgrade permeability of $k_{sat} = 1 \times 10^{-8}$ m/s. In addition, Fig. 16 also compares results from the current investigation to those from Rushton and Ghataora [21] which relate to a drainage solution including a highly permeable geocomposite (1-cm thick with a permeability of 5×10^{-3} m/s) between the

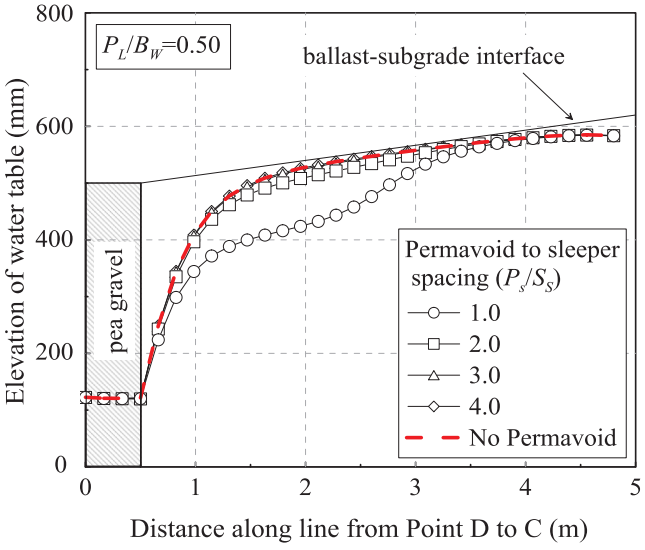

Fig. 15. Effect of drainage unit spacing P_S/S_S on steady-state water table level along line from point D to C.

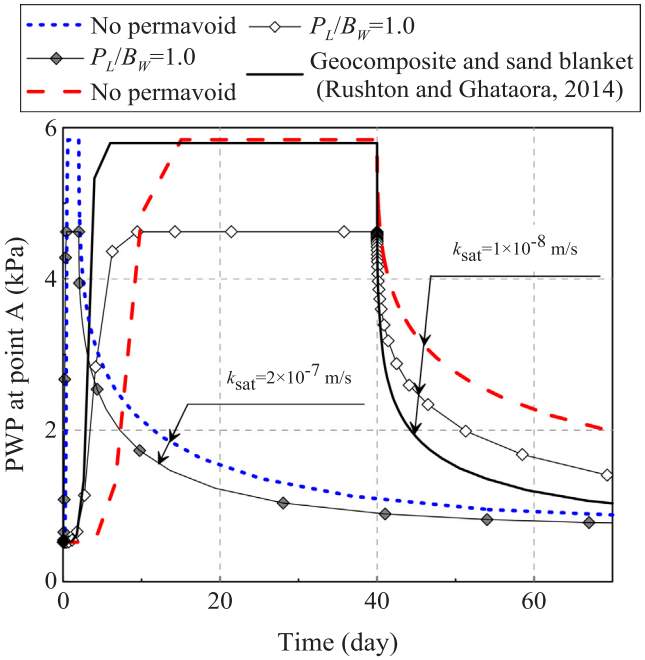

Fig. 16. Effect of subgrade permeability on pore water pressure (PWP) at point A with time; comparison with geocomposite and sand blanket method proposed by Rushton and Ghataora [21].

subgrade and a 10-cm thick sand blanket with a permeability of 2×10^{-5} m/s (placed beneath the ballast). Results show that by decreasing the permeability of the subgrade by an order of magnitude, both the time to reach steady state and the time to dissipate PWP are increased significantly. However, the PWP at steady state is the same for the two cases of subgrade permeability.

Fig. 16 indicates that the PWP at steady state using Permavoid (P_L/B_W = 1.0) is lower than the drainage solution using a geocomposite and sand blanket. Results demonstrate a potentially important feature of the Permavoid drainage solution; it moves the water table away from the ballast-subgrade interface which could ultimately reduce the possibility of mud pumping. The dissipation of PWP after rainfall is noted to be faster for the geocomposite and sand blanket solution proposed by Rushton and Ghataora [21]. This is mainly due to the fact that the

Permavoid only partially covered the width of the model (along BD in Fig. 10), whereas the geocomposite and sand blanket was considered to span the entire width.

Conclusions

A resilient railway infrastructure requires effective and robust drainage systems. This paper presented the results of a study aimed at evaluating the effect of placing geocellular drainage units across the track at the ballast-subgrade interface on the hydraulic performance of the railway track.

The experimental results indicated that the lateral drainage units were effective at reducing the steady-state water level, especially for cases with fouled ballast, and increased the time required to reach the steady-state condition. The open structure of the drainage units enabled fines to migrate downwards from the ballast, with some being washed out into the side drain. In addition, the drainage units maintained the water table below the subgrade-ballast interface in the fouled ballast tests, thereby reducing the likelihood of mud pumping.

The FEM numerical model provided satisfactory agreement with the physical model and was able to capture the correct trend of the transient response of water pressures in the subgrade soil material, including for the effect of unsaturated conditions. The numerical parametric study indicated that the drainage units should extend at least 75% of the distance to the mid-point between tracks in a double-track railway (i.e. $P_L/B_W \geq 0.75$). In terms of spacing along the track, the numerical analyses indicated that the influence of the drainage units is only significant if they are placed between each sleeper.

This investigation only considered the hydraulic behaviour of the drainage units; the mechanical response of these units as well as the railway system as a whole should also be evaluated.

Declaration of Competing Interest

The authors declare that they have no known competing financial interests or personal relationships that could have appeared to influence the work reported in this paper.

Acknowledgments

This study was supported by the Engineering and Physical Sciences Research Council (EPSRC), Rail Safety and Standards Board (RSSB), and Department for Transport (DfT) [EP/M023028/1]. The authors are grateful to Lee Hickling, Andy Maddison, and Luke Bedford for their assistance during laboratory testing.

References

[1] Anbazhagan P, Bharatha TP, Amarajeevi G. Study of ballast fouling in railway track formations. Indian Geotech J 2012;42(2):87–99. https://doi.org/10.1007/s40098-012-0006-6.

[2] Cardoso R, Fernandes V, Ferreira TM, Teixeira PF. Settlement prediction of high speed railway embankments considering the accumulation of wetting and drying cycles. Paper presented at the Unsaturated Soils: Research and Applications, Berlin, Heidelberg; 2012.

[3] Chawla S, Shahu JT. Reinforcement and mud-pumping benefits of geosynthetics in railway tracks: numerical analysis. Geotext Geomembr 2016;44(3):344–57. https://doi.org/10.1016/j.geotexmem.2016.01.006.

[4] Cui YJ, Duong TV, Tang AM, Dupla JC, Calon N, Robinet A. Investigation of the hydro-mechanical behaviour of fouled ballast. J Zhejiang Univ Sci A 2013;14(4):244–55. https://doi.org/10.1631/jzus.A1200337.

[5] Cui YJ, Lamas-Lopez F, Trinh VN, Calon N, D'Aguiar SC, Dupla J-C, et al. Investigation of interlayer soil behaviour by field monitoring. Transp Geotech 2014;1(3):91–105. https://doi.org/10.1016/j.trgeo.2014.04.002.

[6] Danquah WO, Ghataora G, Burrow MPN. The effect of ballast fouling on the hydraulic conductivity of the rail track substructure. In: Paper presented at the 15th Danube - European Conference on Geotechnical Engineering, Vienna, Austria; 2014.

[7] Duong T, Cui Y, Tang A, Dupla J, Canou J, Calon N, et al. Physical model for studying the migration of fine particles in the railway substructure. Geotech Test J 2014;37(5):895–906.

[8] Duong TV, Cui Y-J, Tang AM, Dupla J-C, Calon N. Effect of fine particles on the hydraulic behavior of interlayer soil in railway substructure. Can Geotech J 2014;51(7):735–46. https://doi.org/10.1139/cgj-2013-0170.

[9] Fatahi B, Khabbaz H, Liem Ho H. Effects of geotextiles on drainage performance of ballasted rail tracks. Australian Geomech 2011;46:91.

[10] Gumbel EJ. The return period of flood flows. Ann Math Statist 1941;12(2):163–90. https://doi.org/10.1214/aoms/1177731747.

[11] Heyns FJ. Railway track drainage design techniques Ph.D. Ann Arbor: University of Massachusetts Amherst; 2000.

[12] Huang H, Tutumluer E, Dombrow W. Laboratory characterization of fouled railroad ballast behavior. Transp Res Rec 2009;2117(1):93–101. https://doi.org/10.3141/2117-12.

[13] Hudson A, Watson G, Le Pen L, Powrie W. Remediation of mud pumping on a ballasted railway track. Procedia Eng 2016;143:1043–50. https://doi.org/10.1016/j.proeng.2016.06.103.

[14] Koohmishi M, Palassi M. Effect of gradation of aggregate and size of fouling materials on hydraulic conductivity of sand-fouled railway ballast. Constr Build Mater 2018;167:514–23. https://doi.org/10.1016/j.conbuildmat.2018.02.040.

[15] Latvala J, Nurmikolu A, Luomala H. Problems with railway track drainage in Finland. Procedia Eng 2016;143:1051–8. https://doi.org/10.1016/j.proeng.2016.06.098.

[16] Marinho FAM, Take WA, Tarantino A. Measurement of matric suction using tensiometric and axis translation techniques. Geotech Geol Eng 2008;26(6):615. https://doi.org/10.1007/s10706-008-9201-8.

[17] Network Rail. Railway drainage system manual, Part 2A: General design requirements (NR/L3/CIV/005/2A). London, UK: Network Rail; 2010.

[18] Paiva C, Ferreira M, Ferreira A. Ballast drainage in Brazilian railway infrastructures. Constr Build Mater 2015;92:58–63. https://doi.org/10.1016/j.conbuildmat.2014.06.006.

[19] Parsons RL, Rahman AJ, Han J, Glavinich TE. Track ballast fouling and permeability characterization by using resistivity. Transp Res Rec 2014;2448(1):133–41. https://doi.org/10.3141/2448-16.

[20] Rushton KR, Ghataora G. Understanding and modelling drainage of railway ballast. Proc Inst Civil Eng - Transport 2009;162(4):227–36. https://doi.org/10.1680/tran.2009.162.4.227.

[21] Rushton Ken R, Ghataora Gurmel. Design for efficient drainage of railway track foundations. Proc Inst Civil Eng - Transport 2014;167(1):3–14. https://doi.org/10.1680/tran.11.00023.

[22] Schmidt S, Shah S, Moaveni M, Landry BJ, Tutumluer E, Basye C, et al. Railway ballast permeability and cleaning considerations. Transp Res Rec: J Transp Res Board 2017;2607:24–32. https://doi.org/10.3141/2607-05.

[23] Selig ET, Waters JM. Track geotechnology and substructure management. Telford; 1994.

[24] Su Z, Huang H, Jing G. Experimental analysis permeability characteristics of fouling railway ballast. Metallurg Min Indus 2015;7(9):992–7.

[25] Sussmann T, Ruel M, Chrismer S. Source of ballast fouling and influence considerations for condition assessment criteria. Transp Res Rec: J Transp Res Board 2012;2289:87–94. https://doi.org/10.3141/2289-12.

[26] Tasalloti A, Marshall AM, Heron CM, Hashemi MA. Effect of drainage components on the stiffness of ballast under cyclic loading. In: The XVII European conference on soil mechanics and geotechnical engineering, 1–6 September 2019, Reykjavik, Iceland; 2019.

[27] Tennakoon N, Indraratna B, Rujikiatkamjorn C, Nimbalkar S, Neville T. The Role of ballast-fouling characteristics on the drainage capacity of rail substructure. Geotech Test J 2012;35(4):1–12.

[28] Trani LDO, Indraratna B. Assessment of subballast filtration under cyclic loading. J Geotech Geoenviron Eng 2010;136(11):1519–28. https://doi.org/10.1061/(ASCE)GT.1943-5606.0000384.

[29] Van Genuchten MT. A closed-form equation for predicting the hydraulic conductivity of unsaturated soils 1. Soil Sci Soc Am J 1980;44(5):892–8.